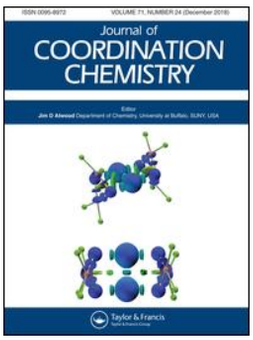

Taylor & Francis
Taylor & Francis Group

Journal of Coordination Chemistry

ISSN: 0095-8972 (Print) 1029-0389 (Online) Journal homepage: https://www.tandfonline.com/loi/gcoo20

Ru(II)-polypyridine complexes with alkynyl Schiff base ligand: influence of π-conjugation, donor/acceptor substituents, and counter anions on electrochemical, luminescence, and catalytic properties

A. B. Patil-Deshmukh, S. S. Mohite & S. S. Chavan

To cite this article: A. B. Patil-Deshmukh, S. S. Mohite & S. S. Chavan (2020): Ru(II)-polypyridine complexes with alkynyl Schiff base ligand: influence of π-conjugation, donor/acceptor substituents, and counter anions on electrochemical, luminescence, and catalytic properties, Journal of Coordination Chemistry, DOI: 10.1080/00958972.2020.1757663

To link to this article: https://doi.org/10.1080/00958972.2020.1757663

Published online: 13 May 2020.

JOURNAL OF COORDINATION CHEMISTRY
https://doi.org/10.1080/00958972.2020.1757663

Ru(II)-polypyridine complexes with alkynyl Schiff base ligand: influence of π-conjugation, donor/acceptor substituents, and counter anions on electrochemical, luminescence, and catalytic properties

A. B. Patil-Deshmukh, S. S. Mohite and S. S. Chavan

Department of Chemistry, Shivaji University, Kolhapur, Maharashtra, India

ABSTRACT

Ru(II)-polypyridine complexes of the general formula $[Ru(L_1/L_2)(phen)_2]X_2$ (**1a–6a**) and $[Ru(L_1/L_2)(bipy)_2]X_2$ (**1b–6b**) (where $X = ClO_4$, BF_4, PF_6; phen = 1,10-phenanthroline, bipy = 2,2′-bipyridine) were prepared by the reaction of $[Ru(phen)_2Cl_2]\cdot 2H_2O$ and $[Ru(bipy)_2Cl_2]\cdot 2H_2O$ with (*E*)-5-((4-methoxyphenyl)ethynyl)-*N*-(pyridin-2-ylmethylene)pyridin-2-amine (L_1) and (*E*)-5-((4-nitrophenyl)ethynyl)-*N*-(pyridin-2-ylmethylene)pyridine-2-amine (L_2) in the presence of $NaBF_4$, $NaClO_4$, and $NaPF_6$. The electrochemical properties of all the complexes indicate reversible redox behavior corresponding to Ru(II)–Ru(III) couple and are susceptible to variation of electron-donating/accepting properties of substituent group on L_1 and L_2. All complexes showed room temperature luminescence corresponding to $\pi \rightarrow \pi^*$ intra-ligand charge-transfer (ILCT) transition with chelation enhanced fluorescence and is finely tuned by increasing π-conjugation, size of counter anions, and variation of substituent group with different electronic effects in the complexes. All the complexes worked as an effective catalyst for the oxidation of benzyl alcohol to corresponding benzaldehyde in good yield at room temperature.

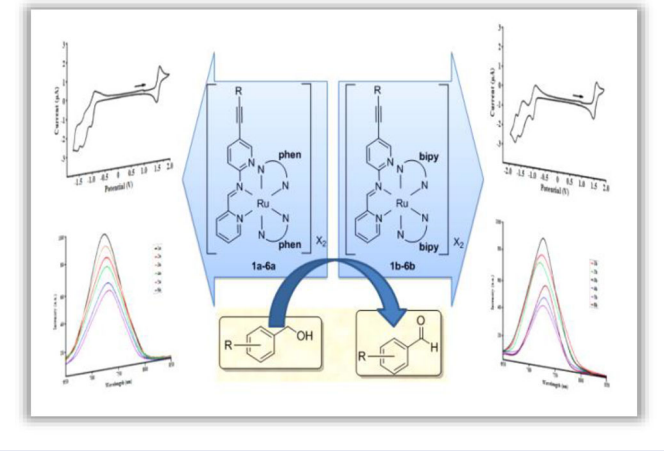

ARTICLE HISTORY
Received 4 December 2019
Accepted 5 April 2020

KEYWORDS
Ru(II) complexes; photoluminescence; cyclic voltammetry; catalytic activity

CONTACT S. S. Chavan sanjaycha2@rediffmail.com Department of Chemistry, Shivaji University, Kolhapur (MS), India 416 004.

1. Introduction

Over the past several decades, large number of ruthenium–polypyridine complexes has been extensively studied due to their unique photophysical and electrochemical properties associated with strong metal–ligand charge-transfer absorption. Several ruthenium–polypyridine complexes have been exploited owing to their potential applications in the synthesis of metallodendrimers, supramolecular assemblies, in analytical chemistry, electrochemistry, ring-opening metathesis, and polymerization [1–4]. They also act as efficient catalysts in a variety of organic transformations such as hydrogenation of esters to alcohols, synthesis of imines from amines and alcohols, the synthesis of amides from amines and esters, and the direct synthesis of polyamides from diamines and diols [5–8]. In recent years, considerable research interest has focused on the development of newer classes of mixed ligand ruthenium–polypyridine complexes by incorporation of desired groups or other types of donor sites which alter the redox and other physicochemical properties of the prepared complexes. The development of these complexes becomes popular because of their potential applications in photochemical conservation of solar energy, molecular electron devices, and as photoactive DNA cleavage agents for therapeutic purposes [9–11]. Furthermore, the presence of counter anions can play a crucial role in unique properties of these complexes, since the anions have many features such as negative charge, size, and geometry. Many compounds of this type such as $[Ru(bipy)_2]^{2+}$ or $[Ru(phen)_2]^{2+}$ with various ligands like pyrroles [12], imidazole-4,5-dicarboxylic acid or biquinoline derivatives [13], and chiral salicylixazolinate [14] have been reported. The Schiff base ligands also have attracted considerable attention for the construction of mixed-ligand transition metal complexes because of their diverse structure and potential applications in various fields [15–17]. Because of great flexibility and diverse structural aspects, a wide range of Schiff bases have been synthesized and their complexation behavior has been studied. Some Schiff bases bearing alkynyl functionality are reported to exhibit excellent luminescence and optical properties [18, 19]. The structural modification of the complexes due to alkynyl functionality causes a large π-delocalization over the coordinating ligand than the regular complexes. Moreover, the rigidity of the structure and the dipole moment of the complexes may thus increase.

In connection with such studies, the present article reports the synthesis of a series of Ru(II)-polypyridine complexes of the type $[Ru(L_1/L_2)(phen)_2]X_2$ (**1a**–**6a**) and $[Ru(L_1/L_2)(bipy)_2]X_2$ (**1b**–**6b**) (where L_1 = (*E*)-5-((4-methoxyphenyl)ethynyl)-*N*-(pyridin-2-ylmethylene)pyridin-2-amine; L_2 = (*E*)-5-((4-nitrophenyl)ethynyl)-*N*-(pyridin-2-ylmethylene)-pyridine-2-amine; X = ClO_4, BF_4, PF_6; phen = 1,10-phenanthroline, bipy = 2,2′-bipyridine) and the study of the effect of newly-introduced group L_1 and L_2 as well as influence of π-conjugation, donor/acceptor substituents, and size of counter ions on the physical and luminescence properties of the complexes. The electrochemical behavior and catalytic properties of the complexes have also been reported.

2. Experimental

2.1. Materials and general methods

All chemicals used were of analytical reagent grade and used without purification. Solvents used for the synthesis were distilled over appropriate drying reagents.

$[Ru(phen)_2]Cl_2$ [20] and $[Ru(bipy)_2]Cl_2$ [21] were prepared according to the literature procedure. *Caution*! Perchlorate salts of metal complexes are potentially explosive. Only small quantities of materials should be prepared and the samples should be handled with care.

Elemental analyses (C, H, and N) were performed on a Thermo Finnigan FLASH EA-112 CHNS analyzer. Electronic absorption spectra were recorded on a Shimadzu UV-3600 spectrophotometer. Infrared spectra were recorded on a Perkin-Elmer FTIR spectrometer as KBr pellets in the 4000–400 cm^{-1} spectral range. ^1H- and ^{13}C-NMR spectra of the samples were measured on a Bruker-300 MHz instrument using TMS $[(CH_3)_4Si]$ as an internal standard. ESI-MS spectra were recorded using a Finnigan LCQ spectrometer. Thermal analysis of the complexes was carried out on a Perkin Elmer thermal analyzer in nitrogen atmosphere at a heating rate of 10 °C min^{-1}. Luminescence properties were measured using a Perkin Elmer LS 55 spectrofluorometer equipped with quartz cuvette of 1-cm path length at room temperature. Cyclic voltammetry measurements were performed on a CH-400A electrochemical analyzer. A standard three electrode system consisting of Pt disk working electrode, Pt wire counter electrode, and Ag/AgCl reference electrode was used. All measurements were carried out in CH_3CN solution at room temperature with scan rate 100 mV s^{-1} using tetrabutylammonium perchlorate (TBAP) as a supporting electrolyte.

2.2. Synthesis of ligands (L_1 and L_2)

To a solution of 5-((4-methoxyphenyl)ethynyl)pyridin-2-amine (1 mmol, 0.224 g) or 5-((4-nitrophenyl)ethynyl)pyridin-2-amine (1 mmol, 0.239 g) in methanol (10 mL), the solution of pyridine-2-carboxyaldehyde (1 mmol, 0.107 g) in CH_2Cl_2 (10 mL) was added and refluxed for 2 h. Completion of reaction was checked by TLC. After evaporation of solvent, the orange solid obtained was washed with petroleum ether, recrystallized from ethanol, and dried *in vacuo*.

L_1: Yield: 90% (0.282 g). Elemental analysis: Calc. for $C_{20}H_{15}N_3O$: C, 76.66; H, 4.82; N, 13.41%. Found: C, 76.59; H, 4.74; N, 13.44%. IR (KBr), ν_{max} (cm^{-1}): 1631 ν(C[dbond]N), 2156 ν(C[tbond]C), 1161 $\nu(OCH_3)$, 3014 $\nu(C[sbond]H)_{arom}$, 1048 $\nu(C[sbond]H)_{arom}$. ^1H-NMR ($CDCl_3$; 300 MHz), δ(ppm): 8.87 (s, 1H, HC[dbond]N), 3.73 (s, 3H, OCH_3), 9.11–9.13 (d, 1H, Ar), 6.66–8.40 (m, 10H, Ar).

L_2: Yield: 87% (0.285 g). Elemental analysis: Calc. for $C_{19}H_{12}N_4O_2$: C, 69.51; H, 3.68; N, 17.06%. Found: C, 69.41; H, 3.63; N, 17.09%. IR (KBr), ν_{max} (cm^{-1}): 1637 ν(C[dbond]N), 2156 ν(C[tbond]C), 1470 $\nu(NO_2)$, 3014 $\nu(C[sbond]H)_{arom}$, 1048 ν(C[sbond]H, arom.bend). ^1H-NMR ($CDCl_3$; 300 MHz), δ (ppm): 8.87 (s, 1H, HC[dbond]N), 9.11–9.13 (d, 1H, Ar), 6.35–8.39 (m, 10H, Ar).

2.3. Synthesis of $[Ru(L_1)(phen)_2](X)_2$ (1a–3a)

To the solution of $[Ru(phen)_2]Cl_2$ (1 mmol, 0.532 g) in dry ethanol (10 mL), L_1 (1 mmol, 0.313 g) in ethanol (10 mL) was added in anaerobic condition and refluxed for 4 h. Then the solvent was evaporated to 5 mL and in that, saturated aqueous solution of

$NaClO_4$/$NaBF_4$/$NaPF_6$ was added. On cooling the reddish brown solid product obtained was filtered, washed well with 1:1 ethanol:water, and dried *in vacuo*.

1a: Yield: 78% (0.682 g). Elemental analysis: Calc. for $RuC_{44}H_{31}N_7ClO_5$: C, 60.45; H, 3.57; N, 11.21%. Found: C, 60.39; H, 3.46; N, 11.27%. ^{1}H-NMR (DMSO; 300 MHz), δ (ppm): 9.33 (s, 1H, HC[dbond]N), 3.73 (s, 3H, OCH_3), 6.61–8.92 (m, 27H, Ar.). IR (KBr), ν_{max} (cm^{-1}): 1583 ν(C[dbond]N), 2169 ν(C[tbond]C), 1159 ν(OCH_3). Λ_m (CH_3CN, Ω^{-1} cm^2 mol^{-1}): 129.19. ESI MS: 774 ([Ru($C_{12}H_8N_2$)$_2$(C_5H_4NHC[dbond]NC_5H_3NC[tbond]C$C_6H_4OCH_3$)]$^+$, 23), 413 ([Ru(C_5H_4NHC[dbond]NC_5H_3NC[tbond]C $C_6H_4OCH_3$)]$^+$, 55), 282 ([C_5H_4NHC[dbond]NC_5H_3NC[tbond]C$C_6H_4OCH_3$]$^+$, 100), 208 ([C_5H_3NC[tbond]CC_6H_4 OCH_3]$^+$, 49).

2a: Yield: 78% (0.672 g). Elemental Analysis: Calc. for $RuC_{44}H_{31}N_7OBF_4$: C, 61.33; H, 3.63; N, 11.38%. Found: C, 61.27; H, 3.54; N, 11.41%. ^{1}H-NMR (DMSO; 300 MHz), δ (ppm): 9.33 (s, 1H, HC[dbond]N), 3.73 (s, 3H, OCH_3), 6.61–8.92 (m, 27H, Ar). IR (KBr), ν_{max} (cm^{-1}): 1583 ν(C[dbond]N), 2169 ν(C[tbond]C), 1159 ν(OCH_3). Λ_m (CH_3CN, Ω^{-1} cm^2 mol^{-1}): 129.03. ESI MS: 774 ([Ru($C_{12}H_8N_2$)$_2$ (C_5H_4NHC[dbond]NC_5H_3NC [tbond]C$C_6H_4OCH_3$)]$^+$, 21), 413 ([Ru(C_5H_4NHC[dbond]N C_5H_3NC[tbond]C$C_6H_4OCH_3$)]$^+$, 59), 282 ([C_5H_4NHC[dbond]NC_5H_3NC[tbond]C$C_6H_4OCH_3$]$^+$, 100), 208 ([C_5H_3N C[tbond] C$C_6H_4OCH_3$]$^+$, 43).

3a: Yield: 78% (0.717 g). Elemental Analysis: Calc. for $RuC_{44}H_{31}$ N_7OPF_6: C, 57.46; H, 3.37; N, 10.66%. Found: C, 57.34; H, 3.28; N, 10.69%. ^{1}H-NMR (DMSO; 300 MHz), δ (ppm): 9.33 (s, 1H, HC[dbond]N), 3.73 (s, 3H, OCH_3), 6.61–8.92 (m, 27H, Ar). IR (KBr), ν_{max} (cm^{-1}): 1583 ν(C[dbond]N), 2169 ν(C[tbond]C), 1159 ν(OCH_3). Λ_m (CH_3CN, Ω^{-1} cm^2 mol^{-1}): 129.34. ESI MS: 774 ([Ru($C_{12}H_8N_2$)$_2$(C_5H_4NHC[dbond]NC_5H_3NC [tbond]C$C_6H_4OCH_3$)]$^+$, 26), 413 ([Ru(C_5H_4NHC[dbond]NC_5H_3NC[tbond]C$C_6H_4OCH_3$)]$^+$, 61), 282 ([C_5H_4NHC[dbond]NC_5H_3NC[tbond]C$C_6H_4OCH_3$]$^+$, 100), 208 ([C_5H_3C[tbond]C $C_6H_4OCH_3$]$^+$, 47).

2.4. Synthesis of [Ru(L_2)(phen)$_2$](X)$_2$ (4a–6a)

Complexes **4a**–**6a** were prepared similar to the procedure performed for the preparation of **1a**–**3a** except that L_1 was replaced by L_2 (1 mmol, 0.328 g).

4a: Yield: 69% (0.613 g). Elemental Analysis: Calc. for $RuC_{43}H_{28}N_8ClO_6$: C, 58.08; H, 3.17; N, 12.60%. Found: C, 57.99; H, 3.11; N, 12.66%. ^{1}H-NMR (DMSO; 300 MHz), δ (ppm): 9.36 (s, 1H, HC[dbond]N), 6.46–8.92 (m, 27H, Ar). IR (KBr), ν_{max} (cm^{-1}): 1587 ν(C[dbond]N), 2169 ν(C[tbond]C). Λ_m (CH_3CN, Ω^{-1} cm^2 mol^{-1}): 129.14. ESI MS: 789 ([Ru($C_{12}H_8N_2$)$_2$(C_5H_4NHC[dbond]NC_5H_3NC[tbond]C$C_6H_4NO_2$)]$^+$, 18), 428 ([Ru(C_5H_4NH C[dbond]NC_5H_3NC[tbond]C$C_6H_4NO_2$]$^+$, 53), 282 ([C_5H_4NHC[dbond]NC_5H_3NC[tbond] C$C_6H_4NO_2$]$^+$, 100), 223 ([C_5H_3NC[tbond]C$C_6H_4NO_2$]$^+$, 48).

5a: Yield: 69% (0.604 g). Elemental Analysis: Calc. for $RuC_{43}H_{28}N_8O_2BF_4$: C, 58.62; H, 322; N, 12.78%. Found: C, 58.88; H, 3.15; N, 12.85%. ^{1}H-NMR (DMSO; 300 MHz), δ (ppm): 9.37 (s, 1H, HC[dbond]N), 6.47–8.92 (m, 27H, Ar). IR (KBr), ν_{max} (cm^{-1}): 1587 ν(C[dbond]N), 2169 ν(C[tbond]C). Λ_m (CH_3CN, Ω^{-1} cm^2 mol^{-1}): 129.09. ESI MS: 789 ([Ru($C_{12}H_8N_2$)$_2$(C_5H_4NHC[dbond]NC_5H_3NC[tbond]C$C_6H_4NO_2$)]$^+$, 17), 428 ([Ru(C_5H_4NHC[d bond]NC_5H_3NC[tbond]C$C_6H_4NO_2$]$^+$, 57), 282 ([C_5H_4NHC[dbond]NC_5H_3NC[tbond]CC_6H_4 NO_2]$^+$, 100), 223 ([C_5H_3NC[tbond]C$C_6H_4NO_2$]$^+$, 46).

6a: Yield: 69% (0.645 g). Elemental Analysis: Calc. for $RuC_{43}H_{28}N_8O_2PF_6$: C, 55.25; H, 3.02; N, 11.99%. Found: C, 55.19; H, 2.89; N, 12.01%. ^{1}H-NMR (DMSO; 300 MHz), δ (ppm): 9.36 (s, 1H, HC[dbond]N), 6.46–8.92 (m, 27H, Ar). IR (KBr), ν_{max} (cm^{-1}): 1587 ν(C[dbond]N), 2169 ν(C[tbond]C). Λ_m (CH_3CN, Ω^{-1} cm^2 mol^{-1}): 129.13. ESI MS: 789 ($[Ru(C_{12}H_8N_2)_2$ $(C_5H_4NHC[dbond]NC_5H_3NC[tbond]CC_6H_4NO_2)]^+$, 21), 428 ($[Ru(C_5H_4NHC$ $[dbond]NC_5H_3NC[tbond]CC_6H_4NO_2]^+$, 63), 282 ($[C_5H_4NHC[dbond]NC_5H_3NC[tbond]$ $CC_6H_4NO_2]^+$, 100), 223 ($[C_5H_3NC[tbond]CC_6H_4NO_2]^+$, 42).

2.5. Synthesis of $[Ru(L_1)(bipy)_2](X)_2$ (1b–3b)

To the solution of $[Ru(bipy)_2]Cl_2$ (1 mmol, 0.484 g) in dry ethanol (10 mL), L_1 (1 mmol, 0.313 g) in ethanol (10 mL) was added in anaerobic condition and refluxed for 4 h. Then solvent was evaporated to 5 mL and in that, saturated aqueous solution of $NaClO_4$/$NaBF_4$/$NaPF_6$ was added. On cooling the reddish brown solid product obtained was filtered, washed well with 1:1 ethanol:water and dried *in vacuo*.

1b: Yield: 69% (0.570 g). Elemental Analysis: Calc. for $RuC_{40}H_{31}N_7ClO_5$: C, 58.15; H, 3.78; N, 11.87%. Found: C, 58.11; H, 3.70; N, 11.93%. ^{1}H-NMR (DMSO; 300 MHz), δ (ppm): 9.33 (s, 1H, HC[dbond]N), 3.78 (s, 3H, OCH_3), 6.61–8.92 (m, 27H, Ar). IR (KBr), ν_{max} (cm^{-1}): 1593 ν(C[dbond]N), 2166 ν(C[tbond]C), 1159 ν(OCH_3). Λ_m (CH_3CN, Ω^{-1} cm^2 mol^{-1}): 131.21. ESI MS: 726 ($[Ru(C_{10}H_8N_2)$ $C_5H_4NHC[dbond]NC_5H_3NC[tbo$ $nd]CC_6H_4OCH_3]^+$, 31), 413 ($[Ru(C_5H_4NHC[dbond]NC_5H_3NC[tbond]CC_6H_4OCH_3)]^+$, 62), 282 ($[C_5H_4NHC[dbond]NC_5H_3NC[tbond]CC_6H_4OCH_3]^+$, 100), 208 ($[C_5H_3NC[tbond]CC_6$ $H_4OCH_3]^+$, 42).

2b: Yield: 69% (0.561 g). Elemental Analysis: Calc. for $RuC_{40}H_{31}N_7OBF_4$: C, 59.05; H, 3.84; N, 12.05%. Found: C, 58.98; H, 3.74; N, 12.12%. ^{1}H-NMR (DMSO; 300 MHz), δ (ppm): 9.33 (s, 1H, HC[dbond]N), 3.77 (s, 3H, OCH_3), 6.61–8.92 (m, 27H, Ar). IR (KBr), ν_{max} (cm^{-1}): 1593 ν(C[dbond]N), 2166 ν(C[tbond]C), 1159 ν(OCH_3). Λ_m (CH_3CN, Ω^{-1} cm^2 mol^{-1}): 131.14. ESI MS: 726 ($[Ru(C_{10}H_8N_2)C_5H_4NHC[dbond]NC_5H_3NC$ $[tbond]CC_6H_4OCH_3]^+$, 28), 413 ($[Ru(C_5H_4NHC[dbond]NC_5H_3NC[tbond]C$ $C_6H_4OCH_3)]^+$, 67), 282 ($[C_5H_4NHC[dbond]NC_5H_3NC[tbond]CC_6H_4OCH_3]^+$, 100), 208 ($[C_5H_3NC[tbond]$ $CC_6H_4OCH_3]^+$, 39).

3b: Yield: 69% (0.601 g). Elemental Analysis: Calc. for $RuC_{40}H_{31}N_7OPF_6$: C, 55.11; H, 3.58; N, 11.25%. Found: C, 55.07; H, 3.51; N, 11.29%. ^{1}H-NMR (DMSO; 300 MHz), δ (ppm): 9.33 (s, 1H, HC[dbond]N), 3.76 (s, 3H, OCH_3), 6.61–8.92 (m, 27H, Ar). IR (KBr), ν_{max} (cm^{-1}): 1593 ν(C[dbond]N), 2166 ν(C[tbond]C), 1159 ν(OCH_3). Λ_m (CH_3CN, Ω^{-1} cm^2 mol^{-1}): 131.21. ESI MS: 726 ($[Ru(C_{10}H_8N_2)C_5H_4NHC[dbond]NC_5$ $H_3NC[tbond]CC_6H_4OCH_3]^+$, 24), 413 ($[Ru(C_5H_4NHC[dbond]NC_5H_3N$ $C[tbond]CC_6H_4OC$ $H_3)]^+$, 54), 282 ($[C_5H_4NHC[dbond]NC_5H_3NC[tbond]CC_6H_4OCH_3]^+$, 100), 208 ($[C_5H_3$ $NC[tbond]CC_6H_4OCH_3]^+$, 40).

2.6. Synthesis of $[Ru(L_2)(bipy)_2](X)_2$ (4b–6b)

Complexes **4b**–**6b** were prepared similar to the procedure performed for the preparation of **1b**–**3b** except that L_1 was replaced by L_2 (1 mmol, 0.328 g).

4b: Yield: 63% (0.530 g). Elemental Analysis: Calc. for $RuC_{39}H_{28}N_8ClO_6$: C, 55.68; H, 3.35; N, 13.32%. Found: C, 55.61; H, 3.30; N, 13.37%. ^{1}H-NMR (DMSO; 300 MHz), δ (ppm): 9.31 (s, 1H, HC[dbond]N), 6.46–8.71 (m, 27H, Ar). IR (KBr), ν_{max} (cm^{-1}): 1599 ν(C[dbond]N), 2166 ν(C[tbond]C). Λ_m (CH_3CN, Ω^{-1} cm^2 mol^{-1}): 129.51. ESI MS: 741 ($[Ru(C_{10}H_8N_2)C_5H_4NHC[dbond]NC_5H_3NC[tbond]CC_6H_4NO_2]^+$, 19), 428 ($[Ru(C_5H_4NHC[dbond]NC_5H_3NC[tbond]CC_6H_4NO_2]^+$, 49), 282 ($[C_5H_4NHC[dbond]NC_5H_3NC[tbond]CC_6H_4NO_2]^+$, 100), 223 ($[C_5H_3NC[tbond]CC_6H_4NO_2]^+$, 51).

5b: Yield: 64% (0.530 g). Elemental Analysis: Calc. for $RuC_{39}H_{28}N_8O_2BF_4$: C, 56.53; H, 3.41; N, 13.52%. Found: C, 56.46; H, 3.30; N, 13.60%. ^{1}H-NMR (DMSO; 300 MHz), δ (ppm): 9.31 (s, 1H, HC[dbond]N), 6.49–8.71 (m, 27H, Ar). IR (KBr), ν_{max} (cm^{-1}): 1599 ν(C[dbond]N), 2166 ν(C[tbond]C). Λ_m (CH_3CN, Ω^{-1} cm^2 mol^{-1}): 129.28. ESI MS: 741 ($[Ru(C_{10}H_8N_2)C_5H_4NHC[dbond]NC_5H_3NC[tbond]CC_6H_4NO_2]^+$, 22), 428 ($[Ru(C_5H_4NHC[dbond]NC_5H_3NC[tbond]CC_6H_4NO_2]^+$, 51), 282 ($[C_5H_4NHC[dbond]NC_5H_3NC[tbond]CC_6H_4NO_2]^+$, 100), 223 ($[C_5H_3NC[tbond]CC_6H_4NO_2]^+$, 40).

6b: Yield: 63% (0.558 g). Elemental Analysis: Calc. for $RuC_{39}H_{28}N_8O_2PF_6$: C, 52.83; H, 3.18; N, 12.64%. Found: C, 52.77; H, 3.09; N, 12.66%. ^{1}H-NMR (DMSO; 300 MHz), δ (ppm): 9.31 (s, 1H, HC[dbond]N), 6.47–8.71 (m, 27H, Ar). IR (KBr), ν_{max} (cm^{-1}): 1599 ν(C[dbond]N), 2166 ν(C[tbond]C). Λ_m (CH_3CN, Ω^{-1} cm^2 mol^{-1}): 129.57. ESI MS: 741 ($[Ru(C_{10}H_8N_2)$ $C_5H_4NHC[dbond]NC_5H_3NC[tbond]CC_6H_4NO_2]^+$, 27), 428 ($[Ru(C_5H_4NHC[dbond]NC_5H_3NC[tbond]CC_6H_4NO_2]^+$, 60), 282 ($[C_5H_4NHC[dbond]NC_5H_3NC[tbond]CC_6H_4NO_2]^+$, 100), 223 $[C_5H_3NC[tbond]CC_6H_4NO_2]^+$, 38).

2.7. General procedure for catalytic oxidation of alcohol

The oxidation of alcohol catalyzed by Ru(II) complexes was carried out according to the following procedure. To a solution of substituted benzyl alcohol (2 mmol) in DMF, NMO (3 mmol) was added followed by addition of **1a**–**6a** and **1b**–**6b** (0.01 mmol). The reaction mixture was stirred at room temperature for 3 h. The mixture was reduced *in vacuo*, the residue was taken up in diethyl ether and was filtered through a bed of silica gel. The purified product obtained was then characterized by IR, ^{1}H-NMR, and ^{13}C-NMR spectra.

3. Results and discussion

3.1. Synthesis and characterization

The starting material 5-(ethynyl)pyridin-2-amine was prepared by using Pd(II)/Cu(I) catalyzed coupling of 5-iodo-2-aminopyridine followed by hydrolysis reaction with KOH in MeOH by following the procedure reported earlier [21]. Further coupling of 5-(ethynyl)pyridin-2-amine with 1-iodo-4-methoxybenzene and 1-iodo-4-nitrobenzene afforded 5-((4-methoxyphenyl)ethynyl)pyridin-2-amine and 5-((4-nitrophenyl)ethynyl)-pyridin-2-amine, respectively. The Schiff base ligands (*E*)-5-((4-methoxyphenyl)ethynyl)-*N*-(pyridin-2-ylmethylene)pyridin-2-amine (L_1) and (*E*)-5-((4-nitrophenyl)ethynyl)-*N*-(pyridin-2-ylmethylene)pyridin-2-amine (L_2) were obtained by the condensation of equimolar amount of 5-((4-methoxyphenyl)ethynyl)pyridin-2-amine and 5-((4-nitrophenyl)ethynyl)pyridin-2-amine with pyridine-2-carboxyaldehyde in excellent yield (Scheme 1).

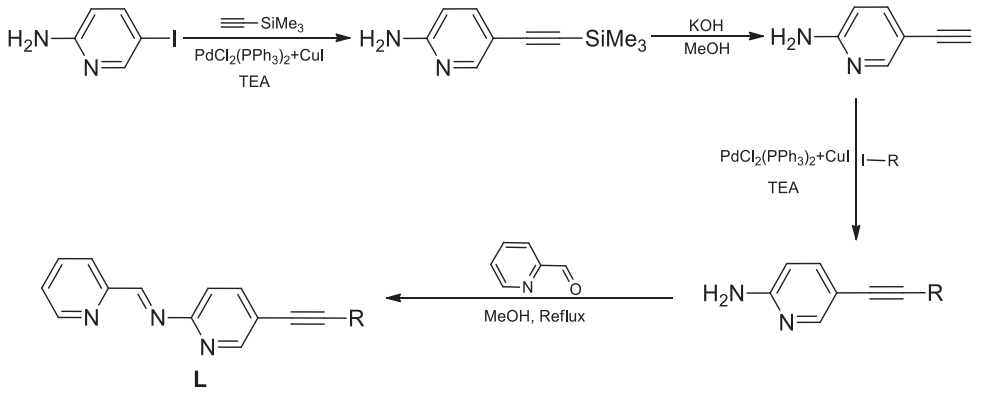

Scheme 1. Synthetic route to the preparation of L_1/L_2.

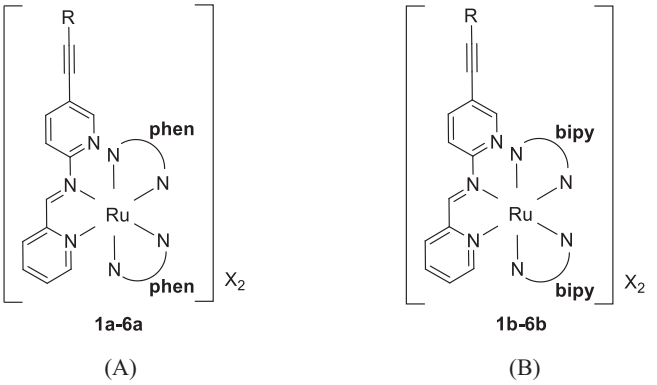

Figure 1. Proposed molecular structure of (A) **1a**–**6a** and (B) **1b**–**6b**.

The mononuclear octahedral complexes of the type $[Ru(phen)_2(NC_5H_4N[dbond]CHC_5H_3C[tbond]CR)]X_2$ (**1a**–**6a**) and $[Ru(bipy)_2(NC_5H_4N[dbond]CHC_5H_3C[tbond]CR)]X_2$ (**1b**–**6b**) were synthesized by the reaction of ethanolic solution of $[Ru(phen)_2Cl_2]\cdot 2H_2O$ and $[Ru(bipy)_2Cl_2]\cdot 2H_2O$ with appropriate ligand L_1/L_2 followed by addition of aqueous NaX solution under N_2 atmosphere (where bipy = 2,2′-bipyridine; phen = 1,10-phenanthroline; R = $C_6H_4OCH_3$, $C_6H_4NO_2$; X = ClO_4^-, BF_4^-, PF_6^-) (Figure 1). The new complexes prepared are air-stable, show great thermal stability, and are moisture-insensitive in solid phase. They are soluble in common organic solvents such as DMF, DMSO, acetonitrile, etc. and their stability in solvent is ensured by ESI-MS spectral studies. Composition and identity of all new compounds were deduced from satisfactory elemental analysis, FTIR, UV–vis, ^{1}H-NMR, ^{13}C-NMR, and mass spectroscopy.

The IR spectra of all the complexes displayed numerous bands of variant intensities. The band at 1586–1599 cm^{-1} in **1a**–**6a** and 1593–1607 cm^{-1} in **1b**–**6b** represents the υ(C[dbond]N) stretching frequency, which is observed at lower frequency region as compared to L_1 and L_2, indicating coordination of (C[dbond]N) group to Ru(II) ion in the complexes [22]. Further proof for the complexation of nitrogen in **1a**–**6a** and **1b**–**6b** is obtained from the appearance of a new band at ca. 491–517 cm^{-1} which is

assignable to ν(M[sbond] N). The pyridine ν(C[sbond]N) observed at ~1603 cm^{-1} in L_1 and L_2 is also shifted to lower frequency by 29–37 cm^{-1} in **1a**–**6a** and **1b**–**6b** [23]. It is to be noted that, upon changing the nature of co-ligand, donor–acceptor groups in Schiff base ligand and counter anions in the complexes appeared to have little effect on the ν(C[dbond]N) frequency. Complexes **1a**–**3a** and **1b**–**3b** exhibit an unsplit band at ~1166 and ~1160 cm^{-1} which are due to $\nu(OCH_3)$ group and two bands at ~1414 and ~1567 cm^{-1} for **4a**–**6a** and ~1410 and ~1560 cm^{-1} for **4b**–**6b**, which can be attributed to ν_{asym} and $\nu_{sym}(NO_2)$ modes, respectively [24]. The IR spectra of **1a**–**6a** are slightly denser as compared to **1b**–**6b** due to more aromatic character of phen ligand relative to bipy. The bands at 519–539 cm^{-1} and 838–839 cm^{-1} are ascribed to the formation of Ru[sbond]N bond from imine and pyridine nitrogen, respectively [25]. The medium strong band at 2156 cm^{-1} in L_1 and L_2 ascribed to stretching frequency of υ(C[tbond]C) was slightly shifted to lower energies after complexation in **1a**–**6a** and **1b**–**6b** suggesting perturbation of the phenyl site leads to electron dissipation at the triple bond through conjugation. The perchlorate complexes **1a**, **4a**, **1b**, and **4 b** exhibit broad band at ~1096 cm^{-1} (ν_3) and unsplit band at ~637 cm^{-1} (ν_4) suggesting the stretching vibration of non-coordinated ClO_4^- ion in the complexes [26]. In tetrafluoroborate complexes **2a**, **5a**, **2b** and **5b**, the intense band at ~1081 cm^{-1} is attributed to the anti-symmetric ν(B[sbond]F) stretching mode [27]. However, strong bands at ~849 cm^{-1} and ~563 cm^{-1} in **3a**, **6a**, **3b**, and **6b** are consistent with the presence of PF_6^- anion in the complexes [28].

The ^{1}H-NMR spectra of L_1 and L_2 exhibit azomethine group resonated at ~8.87 ppm. In the complexes, the signal of azomethine proton is considerably shifted to the downfield region and observed at 9.33–9.37 ppm in **1a**–**6a** and 9.31–9.33 ppm in **1b**–**6b** as a consequence of electron donation to the metal center [29]. The singlet at 3.73 ppm in L_1 is representative of ([sbond]OCH_3) group which did not affect much during complexation. The apparent position of individual proton signals in the aromatic region is not possible because of the ring protons of Schiff base ligand and phen/bipy moieties in **1a**–**6a** and **1b**–**6b** are overlapped in the region 6.46–8.92 ppm. However, the proton counts in the NMR spectra of each of the complexes authenticate the expected structural formulas.

The ^{13}C-NMR spectra of **1a**–**6a** and **1b**–**6b** showed that the coordination also affects the chemical shift of methine group of imine ligands and observed at 167.9–170.97 ppm, while for L_1 and L_2, it appeared at 162.94 ppm and 160.92 ppm, respectively. The signals due to carbon atoms of aromatic ring are observed in the range 115.58–157.84 ppm. The signals of alkynyl group are observed in the range of 97.65–99.13 ppm. This confirms the formation of new Ru(II)-polypyridyl complexes.

3.2. Thermogravimetric analysis

To investigate the thermal stability of **1a**–**6a** and **1b**–**6b**, thermogravimetric analysis (TGA) was performed up to 800 °C under flowing nitrogen at a heating rate of 10 °C min^{-1}. The perchlorate complexes **1a**, **4a**, **1b**, and **4b** are potentially explosive and hence are not studied for safety reasons. The TGA curves of **2a**, **3a**, **2b**, and **3b** show that there is no mass loss up to ca. 187 °C, revealing the absence of either water

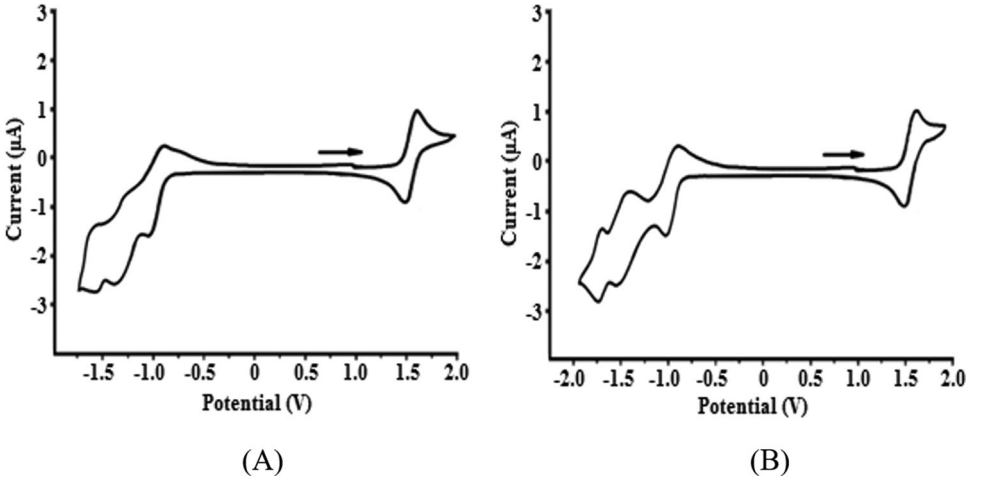

Figure 2. Cyclic voltammograms of (A) **1a** and (B) **1b**.

or solvent molecule. From 187 to 635 °C, these complexes underwent complicated multiple weight loss with total mass loss corresponding to coordinated phen (**2a** and **3a**) or bipy (**2b** and **3b**) ligand, counter anions, and coordinated Schiff base moiety (% obsd. 38.78 (**2a**), 39.42 (**3a**), 36.12 (**2b**), 35.97 (**3b**); % calcd. 38.87 (**2a**), 39.58 (**3a**), 36.38 (**2b**), 35.74 (**3b**)). Complexes **5a**, **6a**, **5b**, and **6b** show very similar behavior to the above; once again the absence of water or solvent molecule indicated and decomposition follow the same stages. Complexes then underwent a rapid and significant weight loss (% obsd. of 42.32 (**5a**), 42.78 (**6a**), 39.38 (**5b**), 38.89 (**6b**); % calcd. 42.57 (**5a**), 42.88 (**6a**), 39.56 (**5b**), 38.69 (**6b**)) from 194 to 644 °C, indicating loss of decomposed coordinated ligands along with counter anions.

3.3. Cyclic voltammetry

The electrochemical properties of **1a**–**6a** and **1b**–**6b** have been studied in CH_3CN solution (10^{-3} M) by cyclic voltammetry using a platinum working electrode. All complexes are electroactive and show one metal-centered oxidation couple as well as one ligand-based and two coligand-based reductions in the potential range of ±2 V *versus* saturated calomel electrode (SCE). The representative voltammograms of **1a** and **1b** are shown in Figure 2 and the electrochemical data are depicted in Table 1. The complexes displayed one reversible couple in the range 1.46–1.53 V for **1a**–**6a** and 1.60–1.69 V for **1b**–**6b** *versus* SCE, which is assigned to the oxidation couple of Ru(II)–Ru(III). The involvement of one Schiff base ligand around Ru(II) ion in the present set of complexes **1a**–**6a** and **1b**–**6b** shifted the Ru(II)–Ru(III) couple to higher values than that of $[Ru(phen)_3]^{2+}$ and $[Ru(bipy)_3]^{2+}$ [30]. This implies that the donor strength of L_1 and L_2 are lower than that of phen and bipy. In addition to the Ru(II)–Ru(III) reversible couple, all complexes displayed three reversible one-electron reductions. The first ligand reduction was at –0.87 to –0.93 V for L_1 and –1.07 to –1.21 for L_2 while the other two were at –1.55 to –1.78 V and –1.61 to –1.79 V for bipy/phen moieties (all potentials are referenced to SCE) [31]. The electrochemical properties

Table 1. Electrochemical data of 1a–6a and 1b–6b[a].

		Ligand reductions		
Complex	Ru^{II}–Ru^{III} couple $E_{1/2}$ (V)[b]	$E_{1/2}$ (V)[b]	$E_{1/2}$ (V)	$E_{1/2}$ (V)
1a	1.47	−0.92	−1.35	−1.55
2a	1.46	−0.93	−1.37	−1.57
3a	1.48	−0.93	−1.36	−1.54
4a	1.51	−1.21	−1.37	−1.57
5a	1.53	−1.17	−1.38	−1.56
6a	1.52	−1.19	−1.41	−1.59
1b	1.60	−0.87	−1.52	−1.68
2b	1.61	−0.92	−1.51	−1.70
3b	1.63	−0.91	−1.54	−1.71
4b	1.67	−1.07	−1.51	−1.70
5b	1.69	−1.14	−1.54	−1.69
6b	1.69	−1.15	−1.55	−1.70

[a]Solvent, acetonitrile; Supporting electrolyte, tetrabutylaminoperchlorate; Reference electrode, SCE; Working electrode, Pt wire.
[b]$E_{1/2} = 0.5(E_{pa} + E_{pc})$, where E_{pa} and E_{pc} are the anodic and cathodic peak potentials, respectively.

correlate well with the nature of substituent groups on the azomethine moiety. The electron donating OCH_3 group cathodically shifts the redox potential in **1a**–**3a** and **1b**–**3b** (Table 1). In contrast, the electron withdrawing NO_2 group induces an appreciable anodic shift in the redox potential of **4a**–**6a** and **4b**–**6b** (Table 1). These results might be due to replacement of [sbond]NO_2 by strong electron donating [sbond]OCH_3 group [32]. 2,2′-Bipyridine is a well-known potential electron-transfer center and each bipy moiety can accept two electrons in one electrochemically accessible LUMO [33]; similarly in phen as well. Since **1a**–**6a** and **1b**–**6b** have two *N*,*N*′-donor units, four one-electron reductions are therefore expected. However, in practice, we have observed two reductions within the ±2 V potential range from bipy and phen. The other expected two reductions could not be seen, possibly due to solvent cut-off. In comparison of the electrochemical data of the prepared complexes it reveals that the redox processes for **1a**–**6a** appeared at slightly more positive potential as compared to those for corresponding **1b**–**6b**. This is attributed to better stabilization of phen-based **1a**–**6a** complexes compared to bipy-based complexes **1b**–**6b** as a consequence of its strong π-acidic character. It is also observed that the $E_{1/2}$ values for **1a**–**6a** are slightly greater than **1b**–**6b** which conclude that the more the π-acidic character the higher the $E_{1/2}$ values.

3.4. Absorption and emission behavior

The electronic absorption spectra of all the complexes were recorded from 200 to 900 nm in CH_3CN solution (10^{-4} M) at room temperature. The spectral data are summarized in Table 2 and the spectra are shown in Figure 3. All ruthenium complexes are diamagnetic, indicating the presence of ruthenium in +2 oxidation state. In **1a**–**6a**, one absorption band around 260 nm is found, which is assigned to the spin-allowed π–π* transitions of the phen ligand. However, **1b**–**6b** show two intense absorption bands around 240 and 290 nm, which are assigned to the typical spin-allowed π–π* transitions of the bipy ligand [34]. For $[Ru(phen)_3]^{2+}$ and $[Ru(bipy)_3]^{2+}$, the lowest energy MLCT transition takes place around 440 and 450 nm, respectively, which is

Table 2. Absorption and emission data of L_1, L_2, 1a–6a and 1b–6b.

Compound	λ_{Abs} (nm)	λ_{Ex} (nm)	λ_{Em} (nm)	ϕ	τ (ns)
L_1	303, 331	272	554	–	–
L_2	311, 342	278	561	–	–
1a	259, 344, 481	291	723	0.0714	6.39
2a	260, 347, 484	298	727	0.0789	6.38
3a	262, 349, 485	293	720	0.0653	6.40
4a	262, 348, 494	299	728	0.0778	6.78
5a	262, 349, 497	298	731	0.0823	6.84
6a	264, 349, 497	296	726	0.0694	6.86
1b	237, 290, 355, 470	296	721	0.0686	6.18
2b	241, 293, 357, 472	291	724	0.0712	6.14
3b	242, 296, 358, 473	295	715	0.0624	6.16
4b	241, 294, 359, 487	295	727	0.0698	6.34
5b	243, 295, 359, 489	291	728	0.0731	6.37
6b	244, 297, 363, 488	296	725	0.0663	6.36

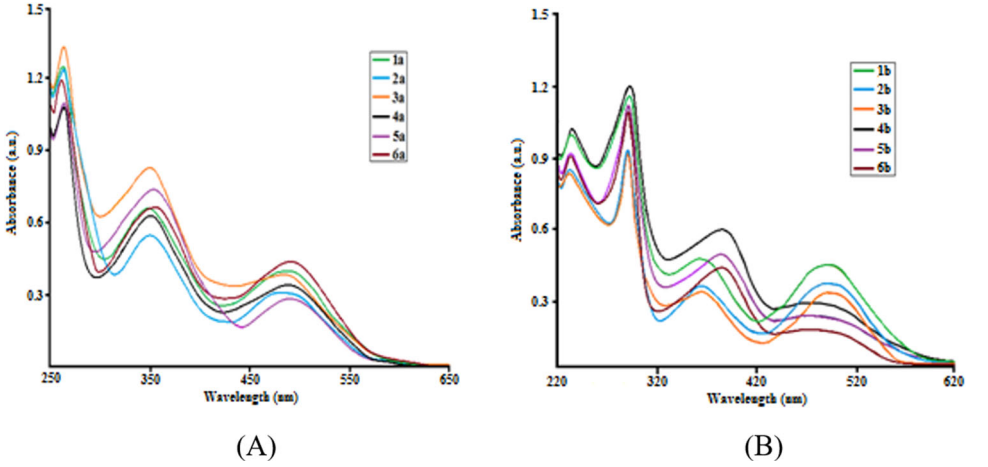

Figure 3. Electronic absorption spectra of (A) **1a**–**6a** and (B) **1b**–**6b**.

reasonably red shifted on substitution of one polypyridine moiety by another *N*,*N*′-donor ligand L_1 and L_2. The most noticeable feature in the visible region of the electronic absorption spectra of the complexes is that, the lowest-energy MLCT maxima are red-shifted with respect to the MLCT of $[Ru(phen)_3]^{2+}$ and $[Ru(bipy)_3]^{2+}$ and the amount of shift depends on the electronic properties of the substituted alkynyl moiety of L [35]. Consequently, the bathochromic shift is observed for **4a**–**6a** and **4b**–**6b** relative to **1a**–**3a** and **1b**–**3b**, which is due to the presence of electron-withdrawing character of the nitro group. Furthermore, compared to **1a**–**6a**, the absorption bands due to MLCT transition appeared at higher wavelength in the spectra of **1b**–**6b**, which may be due to phen ligand showing a strong electron-donating potential than bipy ligand [36]. Little effect of switching the counter ions is also observed on absorption spectra of all the complexes.

Emission spectra of L_1 and L_2 as well as their mixed ligand Ru(II) complexes **1a**–**6a** and **1b**–**6b** were recorded in CH_3CN solution (10^{-4} M) at room temperature and spectral data are displayed in Table 2. The imine alkynyl ligands L_1 and L_2 exhibit emission at 554 nm and 561 nm upon excitation at 272 and 278 nm, respectively. Upon complexation, the mononuclear complexes exhibit strong red-shifted emission at

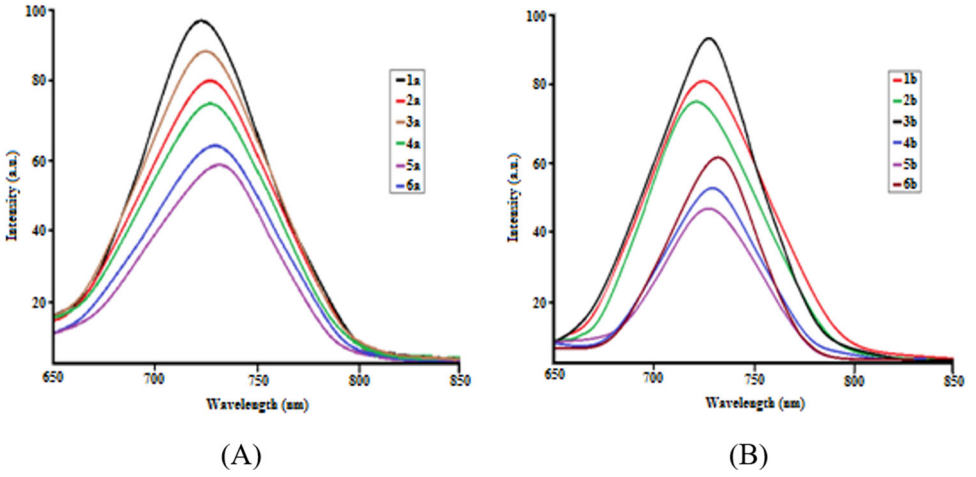

Figure 4. Emission spectra of (A) **1a**–**6a** and (B) **1b**–**6b**.

720–731 nm for **1a**–**6a** and 715–728 nm for **1b**–**6b** with lifetime 6.39–6.86 and 6.18–6.36 ns, respectively (Figure 4). These results confirm that the emission origins in **1a**–**6a** and **1b**–**6b** are predominantly due to $\pi \rightarrow \pi^*$ intra-ligand transition and chelation enhanced fluorescence (CHEF) caused by coordination of imine group to Ru(II) in the complexes [37]. The presence of additional π-conjugation due to Schiff base ligand in **1a**–**6a** and **1b**–**6b** might be one of the important contributing factor for this intense emission, which confirm the chelation of L_1 and L_2. The positive influence on the emission wavelength observed in **4a**–**6a** and **4b**–**6b** is probably a result of the higher electron-withdrawing ability of nitro group which offers an extra conjugated backbone. It was also observed that the fluorescence efficiency of the phen complexes (**1a**–**6a**) appeared at longer wavelength with enhanced intensity as compared to bipy (**1b**–**6b**) complexes. This may be due to the non-radiative decay process which is more effective in the bipy complexes. The presence of counter anion also shows the pronounced effect on the emission behavior of the Ru(II) complexes. When the size of the counter anion increases, the emission wavelength of the Ru(II) complexes decreases and it follows the path $BF_4^- < ClO_4^- < PF_6^-$. These results could be attributed to the difference in coordinating ability of counter anions with Ru(II) ion as well as difference in solubility of the complexes in solution [38].

The emission quantum yield (ϕ) of all the complexes was determined with reference to quinine sulfate ($\phi = 0.52$) and are narrated in Table 2. The appeared quantum yield values are 0.065–0.082 for **1a**–**6a** and 0.062–0.073 for **1b**–**6b**. Compared to $[Ru(phen/bipy)_3]^{2+}$, the significant increase in ϕ value observed for **1a**–**6a** and **1b**–**6b** is probably due to increase in π-conjugation in the complexes. These results are in good agreement with those values reported in the literature [39].

3.5. Catalytic oxidation of alcohol

The synthesized complexes were tested for the oxidation of alcohols to corresponding aldehydes. In order to optimize the reaction conditions such as temperature, solvent, and ratio of the reagents, the oxidation of benzyl alcohol to aldehyde was chosen as

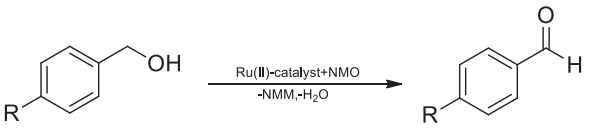

(R = H, CH_3, OCH_3)

Scheme 2. Catalytic oxidation of alcohol.

Table 3. Spectral data of oxidation product.

Compound	IR (cm^{-1})	^{1}H-NMR (ppm)	^{13}C-NMR (ppm)
Benzaldehyde	1702	9.96 (s, [sbond]CHO), 7.86–7.41 (m, 5H)	192.5, 136.2, 134.4, 129.8, 128.9
4-Methyl-benzaldehyde	1701	9.99 (s, [sbond]CHO), 1.16 (s, [sbond]CH_3), 7.87–7.47 (m, 4H)	192.7, 136.2, 134.4, 129.9, 128.9, 21.77
4-Methoxy-benzaldehyde	1698	910.1 (s, [sbond]CHO), 3.78 (s, [sbond]OCH_3), 7.86–7.49 (m, 4H)	193.2, 136.2, 134.4, 129.8, 129.1, 55.56

model reaction and the representative complexes **1a** and **1b** were used as a catalyst. Increasing the temperature of the reaction, no positive effect was observed on the increasing yield of the product. For this reason, all the reactions were carried out at ambient temperature. Using **1a** and **1b** as a catalyst, some other solvents such as CH_3CN and DMSO were examined other than DMF for conversions of alcohol into corresponding aldehydes. Using solvents CH_3CN and DMSO, yields were considerably lowered. Therefore, DMF was used as solvent for subsequent reactions. The ratio of the substrate/catalyst was also optimized and was varied from 1/0.005 to 4/0.005. The ratio of 1/0.005 was chosen because at higher ratios the reaction took a long time to go to completion. Blank experiments were carried out under the same conditions and we observed that the yield of benzaldehyde obtained without the addition of the catalyst was less than 5%, confirming the role of Ru(II) complex catalyst in the catalytic oxidation reaction. Under these optimized conditions, it was observed that **1a**–**6a** and **1b**–**6b** in the presence of NMO as a co-oxidant (Scheme 2) significantly enhance the conversion of benzyl alcohol to desired benzaldehyde in good yield and the product obtained was characterized by IR, ^{1}H-NMR, and ^{13}C-NMR spectra (Table 3). In a typical experiment, a DMF solution of an excess of NMO was added to a stirred solution of an benzyl alcohol and a catalytic amount of Ru(II) complex in DMF. After stirring for 15 min, the red color of the reaction mixture turned brown, probably due to coordination of alcohol to the Ru(II) center. The results obtained for the oxidation of the alcohol by the present catalyst system are summarized in Table 4. By using **1a**–**6a** the oxidation yield of benzaldehyde with benzyl alcohol was observed up to 69%–80%. The oxidation yield of 4-methyl-benzaldehyde with 4-methyl-benzyl alcohol was 75%–84%. However, the oxidation yield of 4-methoxy-benzaldehyde with 4-methoxy-benzyl alcohol considerably increases up to 90%–95%. For **1b**–**6b**, the oxidation yield of benzaldehyde with benzyl alcohol reached up to 61%–67%. However, the oxidation yield of 4-methyl-benzaldehyde with 4-methyl benzyl alcohol and 4-methoxy-benzaldehyde with 4-methoxy-benzyl alcohol was observed up to 67%–77% and 85%–90%,

Table 4. Catalytic oxidation of alcohol by 1a–6a and 1b–6b[a].

Substrate	Product	Catalyst	Yield	Turnover[b]
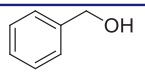	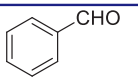	**1a**	79	158
		2a	80	160
		3a	77	154
		4a	69	138
		5a	70	140
		6a	70	140
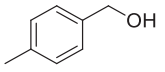	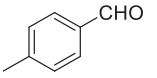	**1a**	84	162
		2a	84	168
		3a	83	166
		4a	77	154
		5a	76	152
		6a	75	150
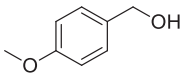	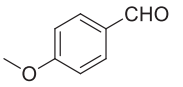	**1a**	93	186
		2a	95	190
		3a	94	188
		4a	90	180
		5a	91	182
		6a	91	182
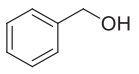	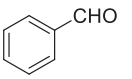	**1b**	64	128
		2b	67	134
		3b	66	132
		4b	61	122
		5b	62	124
		6b	61	122
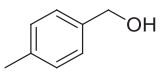	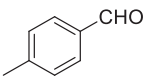	**1b**	76	152
		2b	77	154
		3b	74	148
		4b	69	138
		5b	67	134
		6b	67	134
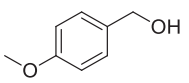	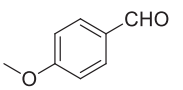	**1b**	89	178
		2b	89	178
		3b	90	180
		4b	87	174
		5b	85	170
		6b	85	170

[a]Reaction conditions: 0.01×10^{-3} M of the complex, 3.0×10^{-3} M of NMO and the substrate 2.0×10^{-3} M were all added to 20 cm^3 of DMF solvent and stirred for 3 h.
[b]Turnover = moles of product/moles of catalyst.

respectively. Following the above study, it was found that the oxidation of electron-donating 4-methoxy-benzyl alcohol transformed readily into corresponding benzaldehyde in excellent yields compared to oxidation of benzyl alcohol and 4-methyl benzyl alcohol [40]. Replacement of non-coordinating counter ions (ClO_4^-, BF_4^-, and PF_6^-) has no major impact on the catalytic activity of **1a**–**6a** and **1b**–**6b**. The donor/accepter nature of imine ligand in the catalyst, however, affects the yield of an oxidation product of benzyl alcohol.

3.6. The mechanism of catalytic oxidation of benzyl alcohol to benzaldehyde by Ru(II) complex

The mechanism suggested here is a process for catalytic oxidation of benzyl alcohol to benzaldehyde by Ru(II) complexes. Results of the present investigations suggest that the complexes are able to react efficiently with NMO to yield a high valent ruthenium-oxo intermediate species capable of oxygen atom transfer to alcohols [41, 42].

The Ru(II) complex reacts with NMO to produce $[Ru^{IV}O(phen)_2(L_1/L_2)]^{2+}$ and $[Ru^{IV}O(bipy)_2(L_1/L_2)]^{2+}$, and the Ru(IV) complex reacts with benzyl alcohol to form $[Ru^{IV}(OH)(PhCH_2O)(phen)_2(L_1/L_2)]^{2+}$ and $[Ru^{IV}(OH)(PhCH_2O)(bipy)_2(L_1/L_2)]^{2+}$, respectively. Afterwards, the hydride ion H^- is abstracted from benzylate anion $PhCH_2O^-$ and then coordinated with ruthenium(IV) to form $[Ru^{IV}(H)(OH)(PhCHO)(phen)_2(L_1/L_2)]^{2+}$ and $[Ru^{IV}(H)(OH)(PhCHO)(bipy)_2(L_1/L_2)]^{2+}$, which is unstable, losing water and giving benzaldehyde according to the following equations:

$$Ru^{II} + NMO \rightarrow Ru^{IV}O + NMM \quad (1)$$

$$Ru^{IV}O + PhCH_2OH \rightarrow Ru^{IV}(OH)(PhCH_2O) \quad (2)$$

$$Ru^{IV}(OH)(PhCH_2O) \rightarrow Ru^{IV}(H)(OH)(PhCHO) \quad (3)$$

$$Ru^{IV}(H)(OH)(PhCHO) \rightarrow Ru^{II} + PhCHO + H_2O \quad (4)$$

4. Conclusion

The mononuclear octahedral complexes of the type $[Ru(phen)_2(NC_5H_4N[dbond]CHC_5H_3C[tbond]CR)]X_2$ (**1a**–**6a**) and $[Ru(bipy)_2(NC_5H_4N[dbond]CHC_5H_3C[tbond]CR)]X_2$ (**1b**–**6b**) were synthesized by the reaction of ethanolic solution of $[Ru(phen)_2Cl_2]\cdot 2H_2O$ and $[Ru(bipy)_2Cl_2]\cdot 2H_2O$ with appropriate ligand L_1/L_2 followed by addition of aqueous NaX solution under N_2 atmosphere (where bipy = 2,2′-bipyridine; phen = 1,10-phenanthroline; R = $C_6H_4OCH_3$, $C_6H_4NO_2$; X = ClO_4^-, BF_4^-, PF_6^-). The phen complexes (**1a**–**6a**) are thermally more stable than the bipy complexes (**1b**–**6b**). All complexes exhibit reversible redox behavior corresponding to Ru(II)/Ru(III) couple and are susceptible to electron donating/accepting properties of the substituent group in the complexes. Further, the redox processes for phen complexes appeared at more positive potential as compared to those for corresponding bipy complexes. Room temperature luminescence is observed for all complexes as a result of intra-ligand $\pi \rightarrow \pi^*$ transition and CHEF. The presence of extended π-conjugation, donor/acceptor substituent on L_1/L_2, π-acidic character of phen and bipy as well as size of counter anions shows pronounced effect on emission properties of the complexes. The catalytic activity of all the complexes in the presence of NMO showed efficient catalytic activity for the oxidation of benzyl alcohol to the corresponding aldehydes at room temperature.

Disclosure statement

No potential conflict of interest statement was reported by the authors.

Funding

One of the authors (ABP-D) is thankful to UGC-BSR-SRF, New Delhi, India for awarding UGC research fellowship in science for meritorious students.

References

[1] P. Govender, A.K. Renfrew, C.M. Clavel, P.J. Dyson, B. Therrien, G.S. Smith. *Dalton Trans.*, **40**, 1158 (2011).
[2] S.H. Toma, M. Uemi, S. Nikolaou, D.M. Tomazela, M.N. Eberlin, H.E. Toma. *Inorg. Chem.*, **43**, 3521 (2004).
[3] A. Demonceau, A.W. Stumpf, E. Saive, A.F. Noels. *Macromolecules*, **30**, 3127 (1997).
[4] J. Suriboot, Y. Hu, T.J. Malinski, H.S. Bazzi, D.E. Bergbreiter. *ACS Omega*, **1**, 714 (2016).
[5] J. Zhang, G. Leitus, Y. Ben-David, D. Milstein. *Angew. Chem. Int. Ed.*, **45**, 1113 (2006).
[6] B. Gnanaprakasam, D. Milstein. *J. Am. Chem. Soc.*, **133**, 1682 (2011).
[7] C. Gunanathan, D. Milstein. *Science*, **341**, 1229712 (2013).
[8] H.X. Zeng, Z.B. Guan. *J. Am. Chem. Soc.*, **133**, 1159 (2011).
[9] M. Yanagida, L.P. Singh, K. Sayama, K. Hara, R. Katoh, A. Islam, H. Sugihara, H. Arakawa, M.K. Nazeeruddin, M. Grätzel. *J. Chem. Soc., Dalton Trans.*, **16**, 2817 (2000).
[10] M. Elvington, J. Brown, S.M. Arachchige, K.J. Brewer. *J. Am. Chem. Soc.*, **129**, 10644 (2007).
[11] S. Rani-Beeram, K. Meyer, A. McCrate, Y. Hong, M. Nielsen, S. Swavey. *Inorg. Chem.*, **47**, 11278 (2008).
[12] T. Lundrigan, C.J.M. Jackson, M.I. Uddin, L.A. Tucker, A.A. Al-Sheikh, A. Linden, T.S. Cameron, A. Thompson. *Can. J. Chem.*, **90**, 693 (2012).
[13] S. Das, D. Saha, C. Bhaumik, S. Dutta, S. Baitalik. *Dalton Trans.*, **39**, 4162 (2010).
[14] R. Borthakur, M. Asthana, A. Kumar, R.A. Lal. *Inorg. Chem. Commun.*, **46**, 198 (2014).
[15] X. Qiu, C. Zhang, S. Li, G. Cao, P. Qu, F. Zhang, J. Ma, B. Zhai. *Inorg. Chem. Commun.*, **46**, 202 (2014).
[16] W. Bi, X. Lu, W. Chai, J. Song, W. Wong, W. Wong, R.A. Jones. *J. Mol. Struct.*, **891**, 450 (2008).
[17] C.K.M. Chan, C. Tao, K. Li, K. Wong, N. Zhu, K. Cheah, V. Yam. *J. Organomet. Chem.*, **696**, 1163 (2011).
[18] S.S. Mohite, A.B. Patil-Deshmukh, S.S. Chavan. *J. Mol. Struct.*, **1176**, 386 (2019).
[19] S.D. Bella, I. Fragala, I. Ledoux, M.A. Diaz-Garcia, T.J. Marks. *J. Am. Chem. Soc.*, **119**, 9550 (1997).
[20] E.C. Johnson, B.P. Sullivan, D.J. Salmon, S.A. Adeyemi, T.J. Meyer. *Inorg. Chem.*, **17**, 2211 (1978).
[21] B.P. Sullivan, D.J. Salmon, T.J. Meyer. *Inorg. Chem.*, **17**, 3334 (1978).
[22] R. Hariram, B.K. Santra, G.K. Lahiri. *J. Organomet. Chem.*, **540**, 155 (1997).
[23] J. Kuduk-Jaworska. *Transit. Met. Chem.*, **19**, 296 (1994).
[24] J. Cisterna, V. Dorcet, C. Manzur, I. Ledoux-Rak, J.-R. Hamon, D. Carrillo. *Inorg. Chim. Acta*, **430**, 82 (2015).
[25] S.R. Lolage, S.B. Pawal, S.S. Chavan. *ChemistrySelect*, **2**, 8052 (2017).
[26] D. Fortin, M. Drouin, M. Turcotte, P.D. Harvey. *J. Am. Chem. Soc.*, **119**, 531 (1997).
[27] C. Liu, S. Yu, D. Li, Z. Liao, X. Sun, H. Xu. *Inorg. Chem.*, **41**, 913 (2002).
[28] H.-Y. Shi, Y.L. Huang, J.K. Sun, J.J. Jiang, Z.X. Luo, H.T. Ling, C.K. Lam, H.Y. Chao. *RSC Adv.*, **5**, 89669 (2015).
[29] B. Pesce. *Nuclear Magnetic Resonance in Chemistry*, p. 174, Academic Press, New York (1965).
[30] (a) A. Ceulemansm, L.G. Vanquickenborne. *J. Am. Chem. Soc.*, **103**, 2238 (1981); (b) M.J. Root, E. Deutsch. *Inorg. Chem.*, **24**, 1464 (1985);(c) R. Alsfasser, R.V. Eldik. *Inorg. Chem.*, **35**, 628 (1996);(d) B.J. Coe, T.J. Meyer, P.C. White. *Inorg. Chem.*, **34**, 593 (1995).
[31] A. Nayak, S. Patra, B. Sarkar, S. Ghumaan, V.G. Puranik, W. Kaim, G.K. Lahiri. *Polyhedron*, **24**, 333 (2005).
[32] S. Takizawa, K. Shimada, Y. Sato, S. Murata. *Inorg. Chem.*, **53**, 2983 (2014).
[33] S. Bhattacharya. *Polyhedron*, **12**, 235 (1993).
[34] Z.M. Wang, S.M. Shen, X.Y. Shen, Y.Q. Xu, A.Q. Jia, Q.F. Zhang. *J. Coord. Chem.*, **69**, 851 (2016).

[35] (a) J.M. Calvert, J.V. Caspar, R.A. Binstead, T.D. Westmoreland, T.J. Meyer. *J. Am. Chem. Soc.*, **104**, 6620 (1982); (b) S.I. Gorelsky, E.S. Dodsworth, A.B.P. Lever, A.A. Vlcek. *Coord. Chem. Rev.*, **174**, 469 (1998);(c) S.I. Gorelsky, A.B.P. Lever. *Coord. Chem. Rev.*, **208**, 153 (2000).
[36] C.J. Wang, W.F. Xu, B.H. Tong, A.Q. Jia, Q.F. Zhang. *J. Coord. Chem.*, **70**, 1617 (2017).
[37] K. Li, Y. Li, J. Tao, L. Liu, L. Wang, H. Hou, A. Tong. *Sci. Rep.*, **5**, 1 (2015).
[38] Y. Zhu, Y. Ma, J. Zhu. *J. Lumin.*, **137**, 198 (2013).
[39] J. Yoshino, N. Kano, T. Kawashima. *Dalton Trans.*, **42**, 15826 (2013).
[40] (a) D. Tan, J. Xie, Q. Li, H. Li, J. Li, H. Li, J. Lang. *Dalton Trans.*, **43**, 14061 (2014); (b) D. Tan, J. Xie, H. Li, M. Zhang, J. Yao, J. Lang. *ChemCatChem*, **9**, 1113 (2017).
[41] S.-I. Murahashi, N. Komiya, Y. Hayashi, T. Kumano. *Pure Appl. Chem.*, **73**, 311 (2001).
[42] K.C. Hansen, Q. Lin, T.M. Aminabhavi. *Faraday Trans.*, **92**, 3643(1996).